User-reconfigured Haptics: Combining User-Reconfiguration and Visual Manipulations to Enhance Dynamic Passive Haptic Experiences for VR

Xinrong Wang
Saarland University
Saarland Informatics Campus (DFKI)
Saarbrücken, Germany
xiwa05@dfki.de

Yu Jiang
Saarland University, Saarland Informatics Campus
Saarbrücken, Germany
yjiang@cs.uni-saarland.de

Martin Schmitz
University of Koblenz
Koblenz, Germany
martin@uni-koblenz.de

Jürgen Steimle
Saarland University, Saarland Informatics Campus
Saarbrücken, Germany
steimle@cs.uni-saarland.de

Antonio Krueger
Saarland Informatics Campus
DFKI
Saarbrücken, Germany
antonio.krueger@dfki.de

Donald Degraen*
HIT Lab NZ
University of Canterbury
Christchurch, New Zealand
donald.degraen@gmail.com

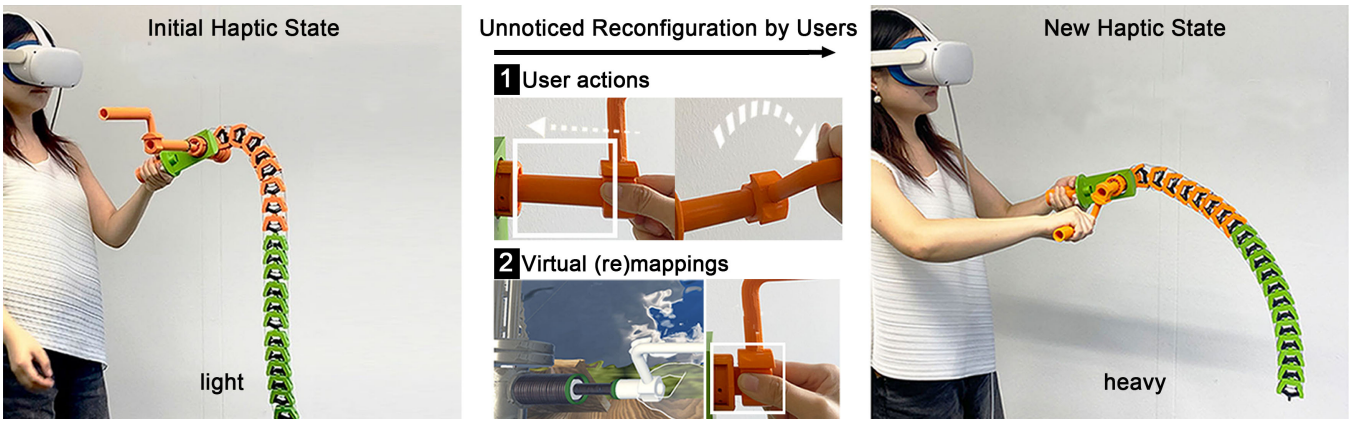

Figure 1: We propose *user-reconfigured haptics*, a haptic feedback concept for Virtual Reality (VR). With our approach, users engage with reconfigurable haptic proxies that can exhibit multiple haptic properties. Users can then transition between these properties without noticing because the act of reconfiguration is masked using virtual (re)mappings. This enables the creation of dynamic virtual experiences supported by user reconfiguration.

Abstract

Virtual Reality (VR) depends on haptic feedback to create immersive experiences. Traditional passive proxies align physical props with their virtual counterparts but remain limited in scalability and expressiveness, or require bulky actuators to support reconfiguration. We introduce *User-reconfigured Haptics*, an approach that utilizes implicit user actions to reconfigure haptic interfaces to extend the gamut of VR haptic experiences. Modular 3D-printed cells are assembled into dynamic interfaces that express diverse haptic properties such as softness and weight. By masking physical reconfigurations with visual (re)mapping, user actions unnoticeably change haptic properties, resulting in user-driven, dynamic haptic experiences. User studies show that our design can provide distinguishable haptic experiences and is perceived as realistic and enjoyable in a VR task. We further showcase four applications: a fishing rod that changes weight and flexibility, a dynamic desktop of pressable buttons, a glove with adjustable squeezing, and a crossbow with variable pulling resistance.

*Corresponding author

CHI '26, Barcelona, Spain

ACM ISBN 979-8-4007-2278-3/26/04
https://doi.org/10.1145/3772318.3793333

CCS Concepts

• **Human-centered computing** → **Haptic devices**; **Virtual reality**; User studies.

Keywords

virtual reality, haptic feedback, user actions, virtual remapping, fabrication

ACM Reference Format:
Xinrong Wang, Yu Jiang, Martin Schmitz, Jürgen Steimle, Antonio Krueger, and Donald Degraen. 2026. User-reconfigured Haptics: Combining User-Reconfiguration and Visual Manipulations to Enhance Dynamic Passive Haptic Experiences for VR. In *Proceedings of the 2026 CHI Conference on Human Factors in Computing Systems (CHI '26), April 13–17, 2026, Barcelona, Spain.* ACM, New York, NY, USA, 16 pages. https://doi.org/10.1145/3772318.3793333

1 Introduction

Virtual Reality (VR) allows users to experience compelling artificially generated worlds. An integral part of such experiences lies in creating realistic sensations of touch. However, providing appropriate haptic feedback for complex VR scenarios where users are freely interacting with a wide range of objects with diverse tactile and kinesthetic properties remains a great challenge [62].

Physical objects can be leveraged as *passive* proxies to simulate virtual touch sensations [24]. Such haptic proxies are inherently limited, as their properties remain unchanged during the virtual experience [61]. This makes them unsuitable for complex scenarios where haptic properties need to change dynamically over time. Strategies that reconfigure physical proxies in real-time can enable a dynamic haptic experience in which the provided haptic feedback changes according to the virtual story [39]. However, this oftentimes requires augmenting proxies with cumbersome actuators. To ensure passive proxies can provide dynamic experiences while remaining lightweight, demand minimum assembly or wiring effort, and considering energy sustainability, researchers have employed external human actors for reconfiguration [5]. Similarly, Cheng et al. [4] proposed to make users themselves dynamically reconfigure a foldable prop or a pendulum, after which the changed physical proxy is visually remapped to a new virtual object to enable a dynamic visuo-haptic experience. However, this approach heavily relies on visually overlaying changing virtual objects and uses existing objects as physical props that provide a limited range of haptic sensations with object-specific reconfiguration actions. This imposes constraints on the expressiveness of the experience they can construct because users need to be constantly redirected away from the proxy while the system visually remaps the proxy.

With *user-reconfigured haptics*, we propose a novel approach that enables a much more flexible user-reconfigured dynamic haptic experience (see Figure 1). We achieve this by introducing modular passive cells that are reconfigurable in shape and elasticity, can be flexibly assembled to create physical proxies with modifiable haptic properties, including softness, shape, weight, flexibility, and pulling resistance. Different types of user action (translation and rotation) native to the VR experience are then exploited to reconfigure the passive haptic proxy to achieve dynamically changing haptic experiences. To realize the implicit reconfiguration by the users themselves, we leverage virtual (re)mapping strategies (one-dimensional (1-D) hand redirection) to mask the needed physical reconfiguration with a virtual action. *User-reconfigured haptics* can realize dynamic haptic experiences that are entirely driven by the user, versatile, and customizable. We demonstrate this with a series of applications, including a fishing rod that changes weight and flexibility perception reconfigured by rod handle manipulations from the user, a tangible shape-changing interface that creates pressable/-touchable buttons dynamically reconfigured by the user switching the virtual interface, a glove that changes shape reconfigured by the user performing the forward and downward stretching action, and a crossbow with changing pulling resistance reconfigured by the user pulling back the bowstring.

We evaluate *user-reconfigured haptics* with a series of user studies, which show that (1) our unit cell design, when stacked in various configurations, can effectively convey distinct variation levels, (2) the virtual (re)mappings can guide user actions, and (3) the entire VR experience with *user-reconfigured haptics* is realistic and enjoyable.

In summary, we make the following contributions:

(1) *user-reconfigured haptics*, which uses reconfigurable haptic proxies with multiple haptic properties, implicit user actions native to VR, and visual (re)mapping strategies to realize dynamic haptic experiences that are passive and driven only by the users themselves;
(2) user studies that show the effectiveness of *user-reconfigured haptics*;
(3) four prototypical applications that demonstrate the feasibility and versatility of our approach.

2 Related Work

Our approach is inspired by research on dynamic haptics, shape-changing structures, and visual distortion strategies.

2.1 Dynamic Haptics

The existing VR community broadly distinguishes between two types of haptic feedback, active haptics and passive haptics. Active haptics typically involves fine-controlled mechanical and electrical systems to deliver dynamic haptic feedback that can promptly adapt to visual changes [64]. Examples include grounded electromechanical pin-array [1] and cable-driven compliant mechanisms [56]. To enhance portability, researchers have developed handheld devices that use fewer actuators while still allowing dynamic haptic feedback [61]. For instance, devices have been successfully created to simulate grasping experiences through motor-driven rings [16], convey weight sensations via center-of-mass shifts [62], and adjust surface areas for kinesthetic feedback [59]. Wearable implementations [32, 34] and modular systems like voxel-based displays [12] and Cubimorph [41] further expand the dynamic capabilities. Though active haptics is promising in providing dynamic haptics, the cost and mechanical complexity tend to scale with the intricacy of the actuation mechanisms [5].

In contrast, the passive haptics leverages low-cost and low-fidelity proxies, typically fabricated through 3D printing or laser cutting [64]. These proxies have emerged as promising interaction interfaces to provide tactile and kinesthetic feedback [62], offering an affordable alternative to the more complex active systems. Passive haptics have been widely employed in various VR applications, as seen in [7, 64] and reconfigurable systems like TanGi, which simulates rotation, stretching, or bending [11]. However, their inability to dynamically reconfigure in response to changing VR experiences limits user presence and immersion in VR [35]. To tackle this, researchers have employed human actuation into passive proxies to enable dynamic experiences [4–6, 29]. In these approaches, users

actively reconfigure passive proxies, guided by VR interactions and narrative cues [4]. However, they typically treat reconfiguration as an explicit meta-task: users rearrange hardware and then resume, with little support for masking these actions or coordinating them with in-scenario interactions. They also tend to target a limited set of properties or shapes per device.

We are inspired by these works and propose *user-reconfigured haptics*, a generic concept that couples shape-changing structures that can be manually reconfigured by users, with visual distortions that guide users to perform these reconfiguration actions so that users' manual reconfigurations happen within the flow of a VR task and directly support multiple haptic properties over time.

2.2 Shape-changing Structures

Shape-changing structures enhance haptic affordances by transforming their shape or materiality in response to user interactions and context [3, 53]. Shape-changing approaches such as linear pin arrays [37, 46], origami [22], kirigami [38], and mesh-based or truss structures [18] have been widely employed to represent digital data tangibly. Although expressive, prototyping such structures usually requires substantial efforts and domain-specific knowledge, resulting in bulky designs [31]. Go beyond designing merely the external macro-scale shape, researchers have explored metamaterials, which use customized micro-scale cells to achieve controlled shape transformations [8, 36]. Metamaterials not only simulate dynamic textures and elasticity [26, 57] but also show great functional potential in developing passive yet interactive mechanisms [25], devices [28, 57], and even computation systems [27]. Metamaterials enable purely manual actuation without electronics, reducing both the complexity and cost of one-off application-specific shape-changing devices [31]. Recent innovations include incorporating compliant components that introduce nonlinear responses and instabilities into metamaterial structures, further enhancing the ability to prescribe controlled shape changes [10, 21, 23].

Among various instabilities, the elastic instability has emerged as a simple yet effective way to achieve controllable shape-changing behaviours [54]. This instability has been investigated in various structures such as hinges, beams, and shells [50, 63]. These elastic structures exhibit large deformations when subjected to moderate forces, allow reversible and rapid return to their initial shape once the load is removed, and can be actuated through simple manual compression [63].

We are inspired by the laterally-constrained elastic beam [20, 30, 63]. We integrated it into our unit cell design, which enables two distinct shape states through simple user actions. These actions can be seamlessly integrated into VR scenarios and then be implicitly driven by visual distortion strategies.

2.3 Visual Distortion Strategies

Visual distortion strategies leverage the dominance of visual cues over proprioceptive signals to reconcile discrepancies between real and virtual haptic properties [13, 14]. By subtly integrating these visual distortions into VR environments, designers can guide users to interact with physical proxies in ways that align with virtual narratives, enhancing both the realism and immersion of VR experiences. This approach has been widely leveraged in VR perception research. For example, fabricated textures overlaid on physical objects have been used to study roughness and hardness perception [9, 19]. Furthermore, haptic re-targeting [62], pseudo-haptics [48], and visuo-haptic illusions [1, 13, 14] have also been utilized to extend dynamic VR perceptions and improve virtual exploration and manipulation capabilities.

These techniques typically serve goals such as shape recognition, input redirection, or extending perceived ranges of a single physical device. In contrast, our focus is on using visual distortion *to support user-driven reconfiguration*. We apply 1-D positional hand redirection along the engagement axis after an aligned start pose, so that a single virtual target can correspond to different physical rings or cell groups. In combination with our modular unit cells, this yields a tight coupling between a passive, user-reconfigurable proxy and visual remapping. To our knowledge, prior user-reconfigurable passive proxies do not integrate such coordinated visual guidance, and prior retargeting / pseudo-haptic work does not provide a modular physical cell for users to assemble.

3 User-Reconfigured Haptics

Dynamic VR scenes often feature objects or tasks whose felt state changes during use (e.g., a tool that becomes heavier, a container that softens as it empties, or a line that tightens under load). Such changing experiences are expressed as perceptual consequences that map to haptic properties (e.g., weight [61, 62], shape [51], stiffness [42, 49], or resistance [52]). While remaining fully passive, user-reconfigured haptics supports a wide range of proxies that exert different haptic properties, ranging from different weights and softnesses to pulling resistance and flexibility. It combines three key elements:

(1) stackable elastic *unit cells* enable the creation of reconfigurable proxies that are capable of providing different haptic properties;
(2) *user actions* drive mechanical transformations in the unit cells that allow users to naturally reconfigure the proxy to transition between different haptic property variations;
(3) integrated *virtual (re)mapping strategies* use visual manipulations to guide these transitions unnoticeably.

In the following, we detail each of these key elements.

3.1 Unit cells

Haptic cues are essential to immersive virtual environments. Prior reconfigurable proxies typically provide discrete kinesthetic and/or tactile haptic properties that are highly dependent on the design of the haptic device and the VR application the proxy is built for, limiting generalizability. In contrast, our user-reconfigured haptics uses modular and stackable unit cells as the fundamental building block to enable various VR haptic properties such as softness, flexibility, or weight.

3.1.1 Unit Cell. When designing the unit cell, we defined several design considerations: (1) the unit cell should be compact yet strong enough; (2) it should deform symmetrically and consistently under typical user input; (3) it should have unified interfaces that allow assemblies to be extended without tools; and (4) these assemblies

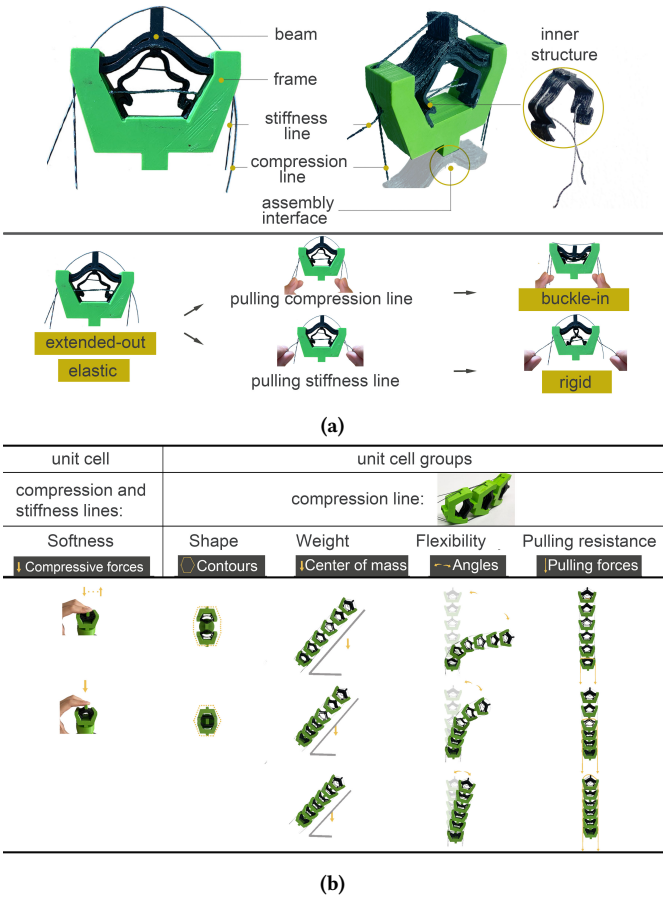

Figure 2: (a). Unit cell structure design. Actuation of the compression line compresses the unit cell, while actuation of the stiffness line alters its mechanical response from elastic to rigid. (b). Unit cell assembly. Multiple unit cells can be combined through fixed interfaces, enabling diverse configurations that map to distinct haptic properties.

should be readily reconfigured by users through simple, natural actions.

As illustrated in Figure 2a, the unit cell comprises three main components: an outer elastic beam structure encased in a rigid frame, an inner compliant insert, and integrated fishing lines for reconfiguration. The outer double-curved beam in a clamped–clamped frame provides symmetric deformation under moderate forces [40]. The inner compliant structure and two fishing lines are further integrated to change the states of the unit cell. As shown in Figure 2a, the unit cell initially exhibits an extended-out and elastic state. Pulling the compression line buckles the outer beams into a buckle-in state. Once the force is released, the unit cell quickly restores to its original form, showing a rapid elastic recovery. Pulling the stiffness line radially tensions the inner insert, collapsing it into a goblet-like form and shifting the unit cell from an elastic to a rigid state. Users feel the cell resists pressure more strongly under stiffness line tension, and releasing the line restores the unit cell to its elastic behavior. This design supports transitions between elastic and rigid and between extended-out and buckle-in, while keeping user actions intuitive (e.g., pulling and pressing).

The unit cell was designed to be largely 3D-printable. For our prototypical implementation, we 3D-printed the outer compliant beam, rigid frame, and inner compliant structure separately, utilizing Prusa i3 MK3S and MINI printers. Testing various filaments (Filaflex 60A, 82A, and 98A) revealed that Filaflex X 82A offered the best balance for the outer beam, while the inner structure was fabricated with 98A to achieve controlled deformation. The rigid frame was fabricated in Prusa PLA and assembled with the compliant beam via an integrated groove connection. This fabrication process ensures precise material performance, enabling our unit cell to function effectively. The parametric information about the unit cell is provided in the supplementary material.

3.1.2 Stackable Unit Cells. A unit cell can be reconfigured via its stiffness and compression lines, allowing users to tune its softness intuitively. When cells are stacked, shared compression lines allow multiple groups to reconfigure simultaneously (see Figure 3 c), expanding the haptic property space. By contrast, driving several stiffness lines at once demands comparatively high tension, which would impose excessive hand effort and a secondary "force-maintain" task. We thus demonstrate stiffness modulation clearly in single-cell use where effort is manageable, and in multi-cell assemblies we prioritize compression-line sharing for simultaneous changes.

In this work, user-reconfigured haptics targets five haptic properties: shape, softness, weight, flexibility, and pulling resistance. These properties are (1) common across dynamic VR scenarios [42, 49, 51, 61, 62], (2) directly controllable with our modular cells and line routing, and (3) support smooth user-driven reconfiguration (other dimensions, such as fine texture, are valuable but out of scope here). As shown in Figure 2b, through unified interfaces, unit cells combine in linear layouts to realize these properties with multiple configurations. These configurations can be further mirrored to represent finer haptic property variations. For instance, a linear chain of six unit cells can selectively compress different subsets to alter the proxy's center of mass, yielding distinct weights. The same chain can modulate internal tension to produce graded pulling resistance. These assemblies broaden the design space of VR proxies while keeping them lightweight and modular.

3.2 User Actions

Whereas dynamic passive haptic feedback utilizes actuators to transition haptic proxies, user-reconfigured haptics builds on the actions of the VR user. These user actions, here, refer specifically to the physical actions that a user is required to do in the VR story—such as twisting, pulling, or pressing—that reconfigure the proxy to provide distinct haptic properties (see Figure 1). Critically seen, these user actions need to be (1) naturally integrated into the VR experience such that the user is not aware that this action is changing the physical proxy, and (2) rough-grained so that the user can easily complete the transition regardless of small errors. When more than two haptic property variations are available, user actions need to be differentiated.

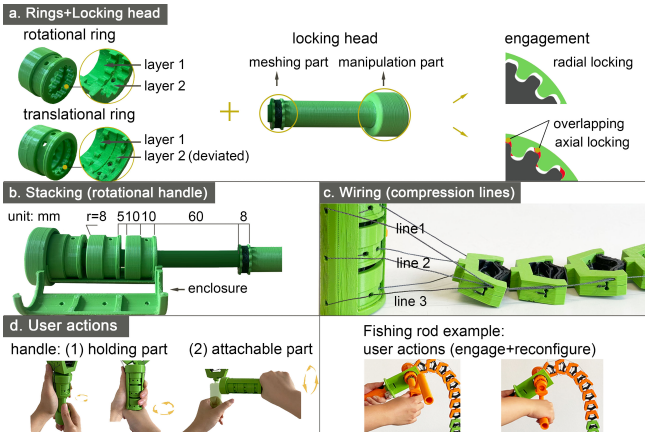

Figure 3: a: The basic structure of the rotational ring, the translational ring, and the locking head. The translational ring's red wedge angle induces self-locking, preventing the locking head from back-driving under press/pull. b. The concentric stacking of rotational rings. c. Wiring layout between rings and unit cells, each ring threads to a compression line controlling a different unit-cell group. d. Possible user actions when grasping the handle, illustrated with the fishing rod example.

We therefore model each action as a two-phase process: In the engagement phase, the user performs an action that defines the next haptic variation to go into. In the reconfiguration phase, the user executes the actual reconfiguration action that changes the proxy. To support this, we propose the translational and rotational reconfiguration mechanisms. These mechanisms build on familiar, task-oriented movements in immersive environments [17, 47], making them versatile and scalable across a wide range of scenarios.

3.2.1 Reconfiguration Mechanisms. As shown in Figure 3 a, both mechanisms share one locking head but rely on different locking rings.

Rotational Ring. As shown in Figure 3 a, two concentric gear layers increase angular tolerance, enabling stable engagement despite minor user deviations. The ring has a toothed band (10 mm) for meshing and a non-toothed band (10 mm) that acts as a transition to lightly twist the head toward the next ring (when stacked). The toothed section features a surface groove to reduce line wear while winding. During the reconfiguration phase, this ring design provides a reliable lock for twisting or bending user actions.

Translational Ring. The translational ring incorporates two staggered, angled gear layers that promote ease of engagement (see Figure 3 a). After the locking head passes the second layer, it tilts between the layers, creating an overlap (wedge) angle that self-locks and prevents reverse slip during pressing or pulling actions. This ring type also features the same 10 mm toothed + 10 mm non-toothed layout.

Locking Head. The meshing part is standardized and partially compliant to mitigate unintended axial shift during engagement, while the user manipulation part is application-specific (e.g., a reel knob). When rings are stacked, passing intermediate rings requires only a small twist/slide; once the target ring is engaged, the head maintains a stable lock throughout the reconfiguration action.

3.2.2 Scalable Reconfiguration Mechanisms. In different VR scenarios, designers (or end users) can select either rotational or translational rings, scale the number of rings, thread each to a specific unit-cell group with a compression line, and stack rings in either planar (horizontal/vertical) (see Figure 8 b) or concentric (co-axial) layouts (see Figure 3 b). The planar layout introduces minimal ring–ring interference, thus the required enclosure can be lightweight and application-specific, just enough to prevent drift. In this stacking layout, the user simply targets a ring and then applies the action.

For the concentric stacking, coaxial rings interact more, so we standardize enclosure design into a **handle** (see Figure 3 b). Here, we describe the rotational handle; the translational one is analogous. The handle integrates an enclosure that houses stacked rings and a shaft that guides the locking head. The holes on the enclosure route compression lines cleanly to avoid tangling (see Figure 3 c). From the user's perspective, the handle lets them select which ring to engage, stabilizes engagement, and transmits their reconfiguration action (e.g., twist) to the targeted cell group.

The handle design is deliberately coarse and tolerant rather than requiring fine alignment. The locking rings provide angular tolerance, and the inter-ring spacing (non-toothed section + ring interval: 15 mm) exceeds the locking-head width (8 mm), which reduces accidental "double engagement" with two rings at once. The enclosure and shaft constrain axial/radial drift, and friction between each ring and the enclosure, as well as between the locking head and the engaged ring, helps the mechanism hold its state after reconfiguration without back-drive. Together, these mechanical features let users focus on the main task (e.g., reeling or lifting) rather than constantly maintaining precise alignment or correcting accidental mis-engagements as a secondary task.

When interacting with this handle, it can be the holding part (see Figure 3 d) to support user actions such as twisting, or an attachable part integrated into a customized holding part (e.g., a reel module on a fishing rod). Note, ring geometry and the locking-head meshing part remain identical across builds; the enclosure/shaft scale, the locking-head manipulation part, and the holding part are customizable to fit different scenarios.

3.3 Virtual (Re)Mapping Strategies

Our approach utilizes virtual (re)mapping and manipulation strategies that alter the user's perception of the virtual environment [39, 45] to implicitly guide users' actions. The goal is twofold: (1) ensure users engage with the intended physical ring so a desired haptic property can be reached, and (2) augment the events occurring in the virtual environment to emphasize the expression of this current haptic property. Here, we focus on remapping in the engagement phase. We use 1-D positional hand redirection [1] to guide the hand to the intended physical ring. Unlike reach-to-touch retargeting [7, 60], our remapping begins after a verified alignment at the start of engagement and does not distort the world or path-plan across objects.

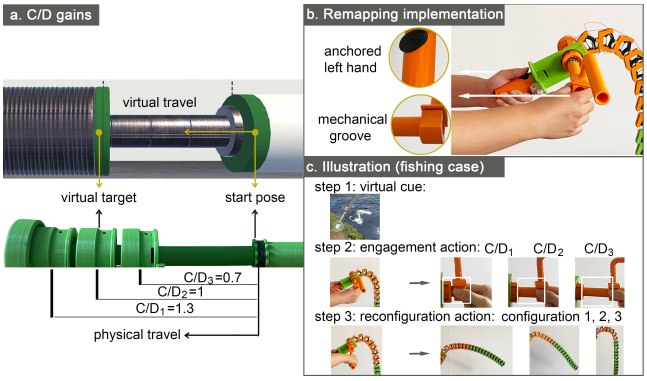

Figure 4: a: Illustration of the visuo-haptic illusion. b. Remapping in a locally anchored frame: we anchor the left hand and update the relative right-hand motion from this verified pose. c. Fishing scenario: (1) a visual cue prompts engagement; (2) varying the C/D ratio engages different physical rings; (3) physical reconfiguration follows, yielding distinct proxy configurations.

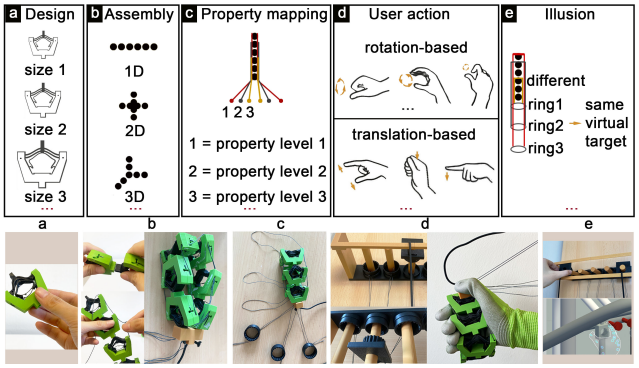

Figure 5: We provide a step-by-step design guidance for creating user-reconfigured haptics and illustrate it with a fitness prototype. From unit-cell design through assembly, haptic-property mapping, user action, and illusion, the workflow is: a. Parametrize unit cells at a nominal size. b. Assemble cells into a linear chain. c. Thread three compression lines through the chain and route each to a distinct translational ring. d. Pair rings with a locking head; the user then performs forward/downward stretches to reconfigure the proxy. e. Apply illusion during engagement to guide ring selection without breaking immersion.

We use the Control/Display (C/D) ratio modification as a mechanism for hand redirection, along the engagement axis. Let the **start pose** be the verified alignment at engagement onset, **virtual target** be the same on-screen goal for all rings, **physical travel** Δx be the change in the hand's physical coordinate from start to ring, and **virtual travel** Δv be the change in the virtual hand from start to the virtual target (see Figure 4 a). Thus C/D = $\frac{\Delta x}{\Delta v}$. Below, we use a fishing-rod with three rotational rings to illustrate the remapping implementation.

We choose the middle ring as reference (C/D = 1) to keep the other gains closer to 1 (e.g., inner ring 1 = 0.7, outer ring 3 = 1.3), avoiding extreme values and making redirection less noticeable. These values lie within reported comfortable ranges for 1-D gains over 70–140 mm travels ($\approx 0.4 - 1.8$) [1, 13], and ensure all rings reach the same virtual target while the physical hand lands at different ring positions.

Prior work often uses markers [7] or trackers [62] to obtain precise free-space hand pose and avoid hand-tracking issues. In our case, we use Oculus Quest hand tracking and run remapping in a locally anchored frame. We snap the virtual rod to the left hand, and enforce left-hand alignment via a simple mechanical groove on the holding part (see Figure 4 b). The right thumb (OVR hand skeleton) is read only after the right hand grasps and aligns with a matching groove on the locking head; we then measure its relative motion from a verified start pose. This avoids free-space estimation: everything is referenced to the left-hand–anchored rod, which reduces global hand tracking drift and reduces the problem to deciding which ring the thumb reaches. Combined with mechanical tolerances (e.g., ring spacing), this makes commodity hand tracking sufficient. If tracking confidence drops, we pause remapping and request realignment before continuing.

Applying remapping in a locally anchored frame scales to different ring counts and layouts (handheld, grounded, and wearable). This strategy makes users' reconfiguration actions unobtrusive and allows multiple proxy configurations to map naturally to distinct haptic properties without breaking immersion (see Figure 4 c).

3.4 Design Process

In this section, we outline a five-step process for authoring user-reconfigured haptics. This process targets VR designers, providing a structured pathway from unit cell design to visual synchronization and guiding designers to create customized proxies while keeping the final implementation both aligned with the current VR content and straightforward for end users to interact with. Designers anticipate the story arc (e.g., Which property should change? Which user action triggers it? How is remapping integrated?) and then follow this pipeline. For clarity and practical relevance, we illustrate with a fitness prototype where users stretch a proxy forward/downward to simulate weight training (see Figure 5).

1. Unit Cell Design: Our unit cell design is highly parametric and scalable, enabling designers to tailor haptic responses for a variety of VR scenarios. Designers first can, if necessary, adjust the unit cells' design parameters (such as thickness, curvature, width, and internal support structures) to fine-tune the mechanical behavior (such as stiffness or compressibility, according to specific haptic goals). Furthermore, the scalable nature of our unit cell allows designers to customize the overall unit cell size to match the current VR content. For example, in the fitness prototype, unit cells were designed at a nominal hand-held size to balance deformability and strength (see Figure 5 a.). In contrast, for a finger-based proxy, designers can minaturize the unit cell to deliver high-resolution feedback that closely mimics natural finger touch sensations. To foster easy modification by designers, we provide all necessary files to modify the design in common CAD tools (such as Rhino).

2. Unit Cell Assembly: Designers can then assemble their individual unit cells into compound structures. Linear chains are efficient for properties like weight, flexibility, and pulling resistance (similar to other reconfigurable haptic toolkits [12]). In the fitness proxy, we built a linear chain as a wearable proxy.

3. Haptic Property Mapping: Once assembled, designers can thread fishing lines through selected cell groups to create distinct property variations. When threading, they should avoid simultaneous multi-stiffness-line pulls and prefer shared compression-line groups for simultaneous reconfiguration. In the fitness prototype, three compression fishing lines were threaded through the chain, enabling three property variations.

4. User Actions: Designers then bind each line/group to a rotational or translational ring. When stacking multiple rings (especially in the handle form factor), designing mechanical tolerances (e.g., ring spacing) enables reliable engagement performance. In the fitness proxy, each compression line is connected to a distinct translational ring.

5. Virtual (Re)Mapping: When stacking rings, designers can apply 1-D positional hand redirection along the engagement axis to ensure reliable engagement with the intended physical ring. They anchor a reference ring (C/D=1) and set gains for other rings accordingly. In our fitness prototype, remapping allows end users to always see the same virtual locking target while tailored C/D gains subtly redirect their hand to different physical rings.

By following this structured process, designers can create reconfigurable proxies that remain versatile across VR contexts, with minute-level assembly once core parts (e.g., unit cells and the handle) are fabricated. As with any toolkit, mis-matching an assembly to the intended feel is possible; the added checks above (e.g., favoring shared compression-line groups for multi-cell changes and designing mechanical spaing for reliable engagement) help keep implementations aligned with the target experience.

4 Example Applications

We showcase the versatility of *user-reconfigured haptics* in creating dynamic VR haptic experiences with four example applications that we implemented prototypically.

4.1 Weight/Flexibility: Fishing

We build a fishing rod that provides changing weight and flexibility haptic feedback with 18 linearly arranged unit cells and a rotational reconfiguration handle. As shown in Figure 6 a, initially, with all unit cells extended, the rod droops, resulting in a center of mass that is very close to the handle. This gives a haptic sensation of a very lightweight fishing rod that corresponds to no fish in the VR scene. While the user bobs the rod by the river, visual cues indicate movement in the water, prompting the user to push laterally to engage the reel and start spinning to reel in the fish. We use C/D ratio manipulations to control the user's push-in distance, transitioning the proxy to different configurations without the user realizing.

After starting the application, the user is first guided to push in 0.7 cm (C/D ratio value=0.7) to transition to the first physical ring. In this state, the reeling in reconfiguration leaves the proxy unchanged, signaling no fish. The user then reels out and pulls out the reel to disengage the fishing rod to continue fishing. Second

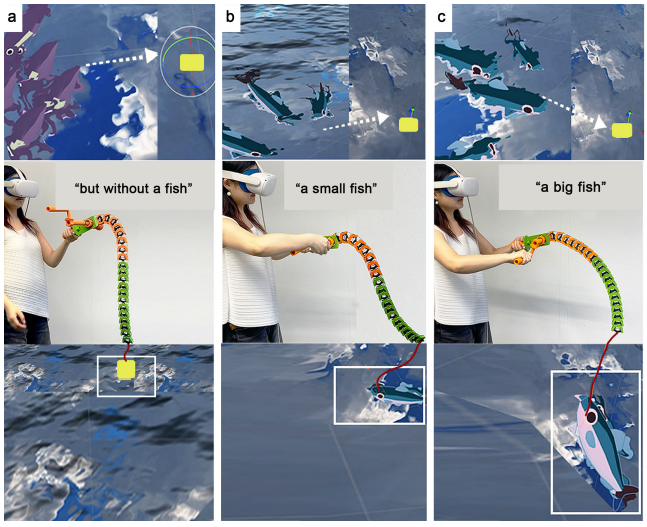

Figure 6: a. In this fishing scene, a user holds a fishing rod and notices movement near the bait. She engages the fishing line and reels in the rod to check if the bait has been taken. As she does so, the rod shifts from a bent to a straight state, though no fish is caught. b. The user notices a cluster of small fish swimming toward the bait. She performs the same push-in and reel-in actions, and then she successfully catches a small fish. c. Afterwards, she catches a big fish.

(see in Figure 6 b), a C/D ratio (value=1) drives a 0.95 cm push and reeling in compresses the first five elastic cells. This shift in the proxy's center of mass makes the rod feel heavier and less flexible, mimicking the sensation of catching a small fish. After taking down the fish, the user reels out and disengages to continue the fishing experience. Third, a 1.2 cm push (C/D=1.3) and reeling in then fully compresses all unit cells (see in Figure 6 c), making the rod feel much heavier and inflexible as the center of mass shifts even further away from the handle and the cells collide with each other, as if reeling in a larger fish.

4.2 Shape/Softness: Tangible virtual interfaces

In this application, we use a four-by-four grounded layout of the unit cells to render haptic feedback for changing virtual interfaces. As illustrated in Figure 7, the user can switch between three virtual interfaces, including playing music, dialing, and gaming, and use one haptic proxy to create corresponding elastic/rigid buttons that can be pressed/touched based on the current interface. The user begins by horizontally moving a white switch to the right and then performs a combined push and rotation on a knob to open the panel cover (see in Figure 7 b). When moving the switch, 1-D hand redirection, modulated by the corresponding C/D ratio, physically drives the user toward a second rotational ring position. When performing the rotation action, the selective buttons pop out (see in Figure 7 c), enabling the user to dynamically experience elastic feedback by pressing push buttons (highlighted in green) to switch songs or adjust volume, or rigid feedback when touching the pause button (highlighted in red).

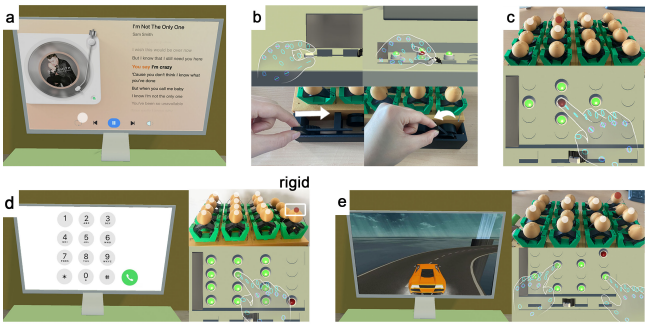

Figure 7: The interface application. a. A user is testing the music interface. b. To open the panel cover, she moves a switch and then performs a combined push and rotation on a knob. During the user's actions, the illusion will physically drive the user to a targeted rotational ring. c. Rotating the ring will activate a unit cell clustering, and the user can then manipulate these cells to perceive varying VR softness experiences. d. The test dialing interface. e. The test gaming interface.

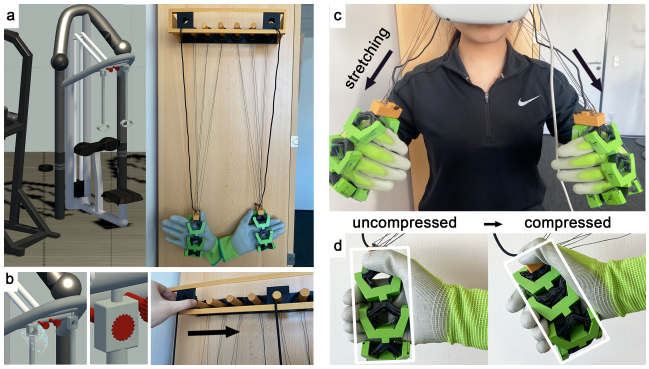

Figure 8: The fitness application. a. The VR scene of the fitness application and the physical wearable proxies. b. Before the fitness, the user moves the stretching module to the right to connect the weight module. c. A user puts on the device and performs the forward and downward action. d. All unit cells change from the uncompressed state to the compressed state, squeezing the user's hand.

Similarly, for the dialing and gaming interface (see in Figure 7 d and e), the same user action masked with visual (re)mappings reconfigure the proxy to create buttons for pressing/touching based on the current virtual interface. By freely switching among the three unit cell clusterings and modulating the unit cells' mechanical responses (elastic or rigid), together with the natural reconfigurable action and virtual (re)mappings, user-reconfigured haptics enables the user to experience varying tactile sensations corresponding to each interface's functional demands.

4.3 Shape: Fitness

The concept of *user-reconfigured haptics* can also be utilized to enhance training experiences in VR exercise scenarios. As shown in Figure 8, we developed a VR fitness application in which the proxy can create changing pressure feedback to simulate different weights that the user is currently pulling. The proxy is made up of 6 linearly connected unit cells that route around a glove. During the forward and downward stretching action (see in Figure 8 d), the shape of the proxy is changed, making it looser or tighter around the hand to deliver varying pressure feedback. resulting in distinct VR weight experiences. Before a back-stretch exercise, the user slides the stretching module to the right to lock the red weight module (see in Figure 8 b). In this setup, the pre-determined C/D ratio guides the user to the designated first translational ring that compresses all unit cells. Once locked and the band is worn, the user experiences a pronounced squeezing sensation during the stretch that simulates a heavier load (see in Figure 8 c). The user then releases the band and adjusts the weight module. This time, the user executes the same action, and the C/D ratio directs the user to a third translational ring, where only a subset of the unit cells is compressed. As a result, the same stretching action yields a lower squeezing sensation, simulating a lighter load.

4.4 Pulling resistance: Crossbow with different sizes

In addition to enriching the VR experiences when one proxy is mapped to one virtual object, *user-reconfigured haptics* also supports 1_to_N mapping. To highlight this potential, we developed the crossbow practice scenario (see in Figure 9) to enrich user interaction and training. The proxy is linearly (7 unit cells) configured to provide changing pulling resistance/force experiences on the bowstring, enabling the same proxy to be mapped to crossbows of varying sizes. In this application, the user practices with three crossbows, which are transported on a conveyor belt into a designated red preparation area. For the largest crossbow, the user engages the system by grasping a board switch with the left hand while the right hand moves forward to position a sight that clamps both the arrow's red tip and the bowstring (see in Figure 9 b). Then the user pulls back to simulate the full draw, during which the user performs the actual reconfiguration action. During the forward movement, the hand redirection guides the user, via the corresponding C/D ratio, to engage with the first translational ring, where full compression of the unit cells is achieved. This reconfiguration facilitates the user to experience the maximum pulling distance and pulling resistance/force, followed by a strong recoil sensation on the left hand upon elastic recovery (see in Figure 9 d).

After completing the first crossbow practice, the user leaves the station, and the conveyor moves the medium-sized crossbow into the target area. As the user proceeds to practice, the same action is performed; however, the C/D ratio now guides the user to the second translational ring, resulting in a partial unit cell compression and a reduced pulling distance and pulling force. Similarly, the proxy can be mapped to the smallest crossbow to experience only a small pulling resistance. This demonstration underscores the ability of our concept to enable a single proxy to represent multiple virtual objects with differing haptic feedback.

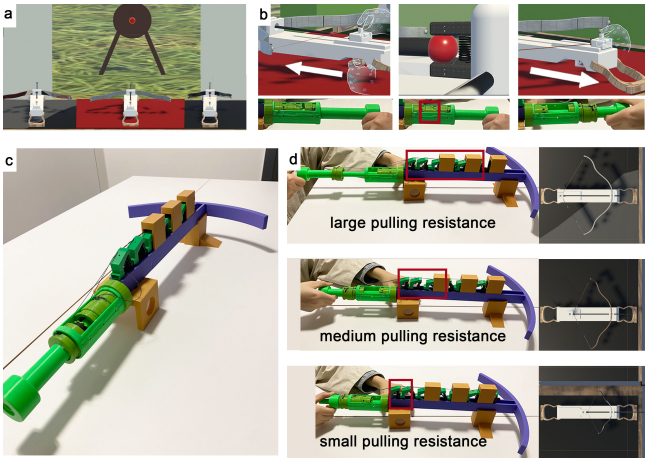

Figure 9: The crossbow application. a. The VR scene of crossbow application. b. From left to right, a user pushes the sight to clamp the bowstring and pulls these components for shooting. c. The crossbow prototype. d. One user is performing the shooting practice; the same proxy can be mapped to crossbows of varying sizes. The red boxes highlight the state of the compressed unit cells under different conditions.

Figure 10: (a) Test setup primarily features a force gauge, a torque wrench, and multiple unit cells. (b) Three testing conditions: with a rotational mechanism, with a translational mechanism, and without any mechanism.

5 Evaluation

In this section, we first quantify the forces generated by different unit-cell arrangements, then report three user studies. Study 1 tests whether users can reliably distinguish between our haptic property variations; Study 2 evaluates whether visual (re)mapping guides users to the correct locking ring for translational and rotational mechanisms; Study 3 explores how the integrated system is experienced in a fishing scenario.

5.1 Technical Evaluation: Forces

In this evaluation, our central interest lies in uncovering a universal relationship between the required reconfiguration force (torque) and the desired reconfiguration.

5.1.1 Procedure. We evaluated how the number of unit cells and the choice of reconfiguration mechanism affect the user force (or torque) required to trigger reconfiguration. We collected data by independently varying: (1) the number of unit cells (one, two, three, five, and ten) and (2) the type of reconfiguration mechanisms (rotational, translational, or none). For each condition, we measured the force (torque) on the compression/stiffness lines using a test setup as shown in Figure 10, primarily featuring a force gauge (Baoshishan ZP-50N with 0.01 N accuracy) and a torque wrench (VANPO Digital Torque Wrench 3/8 Inch with ± 0.02 N · m accuracy). For a single unit cell, we primarily characterized the reconfiguration force (torque) needed to switch between the elastic and rigid states (on the stiffness line). For multiple unit cells, we further characterized the force (torque) required to transition all unit cells from an extended-out state to a buckle-in state (on the compression line).

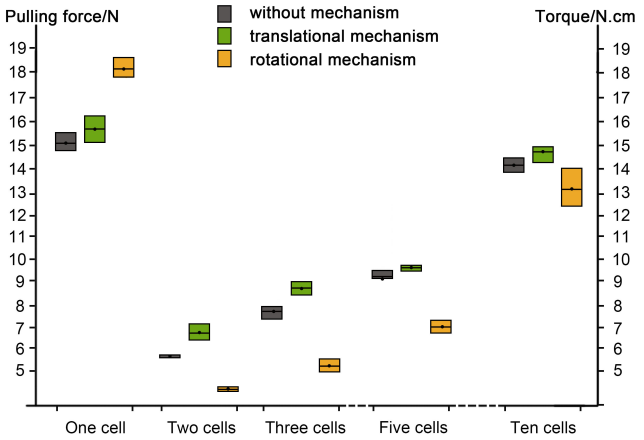

Figure 11: The results of the technical evaluation. When stacking, a general trend where the required reconfiguration force (torque) scales approximately linearly with the number of unit cells is characterized.

5.1.2 Results. Results are presented as a box plot with the crosses highlighting the means in Figure 11. With no mechanism, a single cell required ≈ 15.1 N on the stiffness line to reach a rigid state—within comfortable hand forces for brief actions [58]. Adding a translational mechanism increased the required force slightly (≈ 15.7 N; small added friction). Interpreting torque with the ring radius (r=8 mm) gives an equivalent linear force (≈ 18.3 N) for comparison. Across chains, the required force/torque on the compression line scaled approximately linearly with cell count, with an incremental addition of 1–1.2 N (or N · cm) per unit cell. Tensioning the stiffness line requires relatively high input because (1) it must laterally collapse the inner insert and fully seat the "goblet"

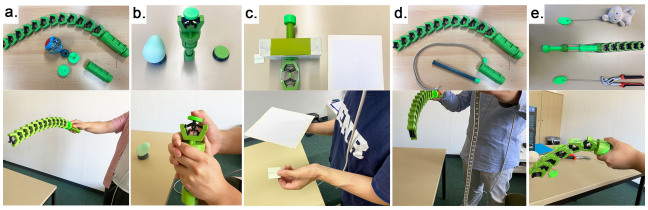

Figure 12: Five prototypes and their corresponding references are prepared to evaluate the haptic property. a. Weight evaluation. b. Softness evaluation. c. Shape evaluation. d. Flexibility evaluation. e. Pulling resistance evaluation.

geometry, and (2) friction along the line path (guides, sheaves, enclosure contacts) adds load; accordingly, we recommend stiffness modulation for single-cell use rather than simultaneous multi-cell changes.

5.1.3 Conclusion. Our findings indicate that the required effort increases roughly with cell count and the mechanism choice adds a small constant offset (friction). Even at 10 cells, values remained within feasible hand forces for short interactions. While linear scaling held in our setup, other unit cell layouts and ring stackings may change absolute values; further exploration is needed in the future.

5.2 User Evaluation 1: Haptic Properties

In this user study, we tested, for each claimed haptic property, whether participants could reliably distinguish among its variations.

5.2.1 Participants. Across studies 1–3 we recruited 14 participants (4 female, 10 male; 24–36 years, M=27.1, SD=4.17) from our university. Twelve participants completed all three evaluations; two additional participants joined Study 3 only. Participants with backgrounds in Computer Science (11), Mathematics (2), and Business Administration (1). All were right-handed, reported normal or corrected-to-normal visual perception, and had no haptic perception issues. Participants had varied VR experiences (6 were novices, 7 used VR annually, and 1 used VR monthly). The study received ethical approval from this university.

5.2.2 Design. We employed a within-subjects design where each participant experienced five types of haptic property (each represented by at least two distinct variations). The independent variables were the haptic property and its variation levels, and the dependent variable was participants' haptic rating on a 10-level scale.

5.2.3 Apparatus. We prepared five prototypes featuring different unit cell numbers and arrangements to simulate different haptic properties (see Figure 12). For each property, we provided two reference objects for the extremes (level 1 and 10 on the scale).

5.2.4 Procedure. Our user evaluation took place in a quiet room. Participants were given a brief introduction to this evaluation and were informed to fill out a consent form and a demographic form.

Participants were blindfolded. Before formal trials, they underwent a training trial. Figure 12 shows the user evaluation scenes.

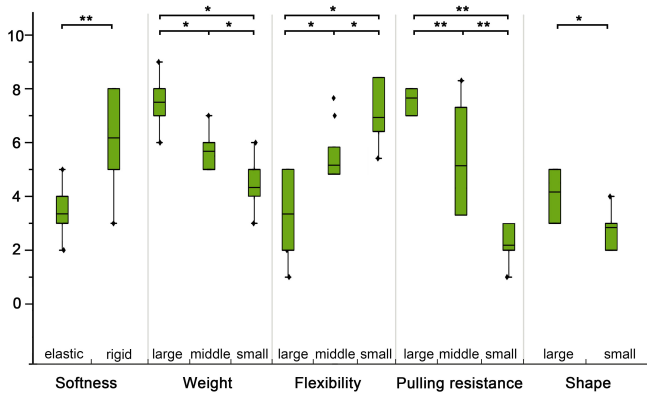

Figure 13: Box plot of haptic property evaluation results, where the crosses highlight the means of each haptic variation. Brackets indicate statistically significant differences, where ⋆ represents p < .05 and ⋆⋆ represents p < . 001.

For each property, participants were first given two reference objects to gauge the haptic property extremes (1 = low end, 10 = high end). Then, participants were handed the test prototype and were asked to rate the haptic expression it provided on a 10-point scale. Instructions and questions were property-specific, e.g., Weight: 'Lift the object; 1 = lightest, 10 = heaviest; Question: how heavy do you think the object is?' and Flexibility: 'Bend/waggle the object; 1 = most flexible, 10 = least; Question: how flexible do you think the object is?' Participants were allowed to refer back to reference objects anytime. The property order was Latin-square counterbalanced and the variant handover order within each property was randomized. After all trials, participants had a short interview.

5.2.5 Results. The results are shown in Figure 13. We outlined the key results of the haptic property evaluation. Overall, participants provided positive feedback on various haptic properties. Significant differences were found in softness (two haptic variations), weight (three haptic variations), flexibility (three haptic variations), pulling resistance (three haptic variations), and shape (two haptic variations). Additional statistical information on each haptic property is available in the supplementary materials.

We further analyzed the audio recordings. Results revealed that differences in softness, shape, and pulling resistance were consistently discernible. For the weight property, 9 out of 12 participants noted clear differences between different haptic variations, participants stated, for example, that *"I thought there were clear differences between three test objects (haptic variations)"* [P4], while another commented, *"...the differences were straightforward and I did not need a lot of time to make my decisions"* [P6]. Feedback on flexibility was also positive; nearly all participants (10 out of 12) found the flexibility haptic variations to be in line with the intended levels. Participants commented, *"I felt these three test objects (haptic variations) were too different-some felt like a hinge while others were more like an elastic-plastic rod"* [P8].

5.2.6 Conclusion. These findings indicate that our proposed unit cell, when stacked in various configurations, effectively conveys

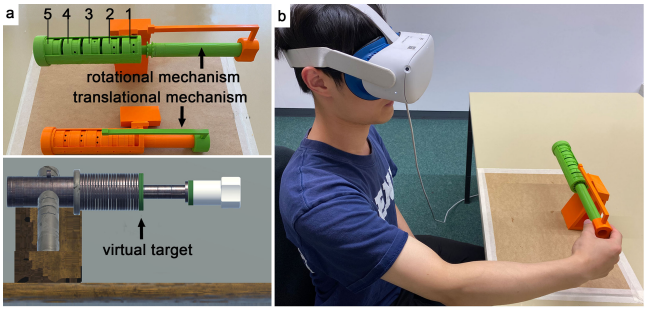

Figure 14: Haptic setup used in the user study. a. The 3D-printed two reconfiguration mechanisms and the virtual counterpart. Each mechanism has five locking rings on the left and a locking head on the right. The virtual counterpart features a green virtual target on the left and a white handle on the right. b. A user is interacting with the rotational mechanism.

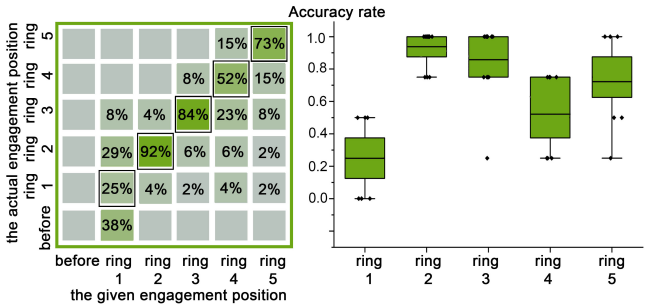

Figure 15: Accuracy rate results of the rotational mechanism. (a) Confusion matrices show the frequency with which each given engagement position is correctly matched by the actual engagement position. (b) Box plot of accuracy rate results, where the crosses highlight the means of accuracy rates for each ring.

distinct haptic properties. Moreover, enhancing a specific haptic variation appears feasible by increasing the number of stacked unit cells.

5.3 User Evaluation 2: Virtual (Re)Mappings

In this study, we evaluated how effectively virtual (re)mapping guided users to engage the correct locking ring for both translational and rotational mechanisms.

5.3.1 Design. We employed a within-subjects design. Each participant completed both mechanisms (order counterbalanced AB/BA across participants). For each mechanism, participants tested five engagement positions ("rings") four times each (20 trials per mechanism). To reduce order effects, we used Latin-square–style counterbalancing for the first repetition: the five rings (1–5) were ordered according to one of five sequences derived from a 5×5 Latin square. These five sequences were assigned cyclically to participants. For the remaining three repetitions within each mechanism, ring orders were pseudo-randomized with the constraints that all rings appeared once per repetition. The dependent variables were accuracy and completion time (from grasp to reaching the virtual target) for each test engagement position.

5.3.2 Apparatus. We prepared 3D-printed prototypes for both mechanisms (see Figure 14). For both mechanisms, we anchored the middle ring (ring 3) at C/D = 1.0 and set gains for the others accordingly (ring 1 = 0.6, ring 2 = 0.8, ring 4 = 1.2, ring 5 = 1.4). These keep gains within commonly reported comfortable ranges for 1-D redirection. We further implemented a customized VR scene built in the Unity game engine (v2021.3.34.f1). Four key functional modules were developed: an automatic calibration module, a movement update module, a data transfer module, and a manager module, ensuring precise spatial registration and data collection. Specifically,

(1) The **automatic calibration module** ensures the spatial registration between physical mechanisms and the virtual counterpart.

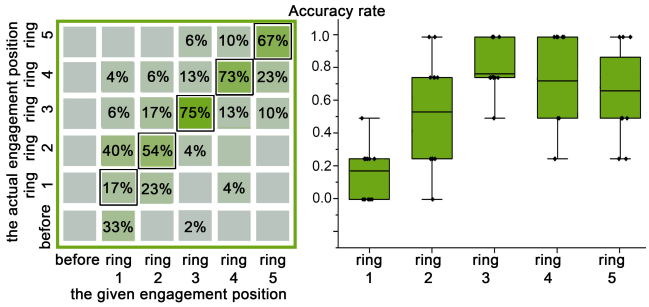

Figure 16: Accuracy rate results of the translational mechanism. (a) Confusion matrices show the frequency with which each given engagement position is correctly matched by the actual engagement position. (b) Box plot of accuracy rate results, where the crosses highlight the means of accuracy rates for each ring.

(2) The **movement update module** integrates the Unity-Oculus package, allowing real-time thumb tracking, ensuring that the virtual handle position updates in sync with the movement of the physical hand.
(3) The **data transfer module** collects metrics such as completion time for analysis.
(4) The **manager module** coordinates all modules.

For rendering, we used a Meta Quest 2 (Meta, formerly Facebook, 2022, build version 33.0) head-mounted display (HMD) in a tethered Oculus Link setup, along with a PC with an AMD Radeon 680M graphics card to immerse participants visually and auditorily.

5.3.3 Procedure. Participants wore an Oculus Quest 2. The virtual counterpart was positioned once at the experiment setup to match the physical device's location, and this global placement remained fixed across trials. The user then started with a calibration: the right thumb (OVR hand skeleton) was aligned to the locking-head groove on the physical device. When the alignment is stably detected, we

record that pose as the start of the engagement axis, and all subsequent thumb motion is measured as a 1-D displacement from this start pose along the ring axis. Upon completion of the calibration, participants performed five practice trials to familiarize themselves with the procedure. Each trial specified a target physical ring, and participants were asked to move along the axis to the same virtual target on screen and then return to the start. Trial and mechanism orders were counterbalanced as described in the Design. After all trials, participants provided brief comments in a short interview.

5.3.4 Results. We described the general findings of the virtual (re)mapping evaluation. Further statistical details about accuracy and completion time are provided in the supplementary materials.

Accuracy. Accuracy results are illustrated in Figure 15 and Figure 16. Overall, for both reconfiguration mechanisms, remapping ensured correct ring engagements across mid-range C/D gains; accuracy decreased near the lowest gain, and the perceived mismatch increased at the highest gain. At Ring 1 (smallest C/D), the same on-screen target is reached with less physical travel. Participants often stopped when the virtual hand hit the target, while the locking head had not yet fully engaged with the physical ring. This low accuracy is primarily attributed to hand-tracking limitations and user action dynamics: at the start of engagement, stacked rings require a small twist, so thumb-tracking jitter plus that micro-motion can satisfy the virtual target too early, prompting participants to stop before the head fully engages. This phenomenon is evident in the confusion matrices shown in Figure 15 and Figure 16. In contrast, ring 5 was accurate yet more noticeable. Although a 1-D C/D gain around 1.4 is often reported as tolerable, our case differs from prior bare-hand movement tasks [1]: the hand grasped the proxy with mechanical contact, which heightens proprioception. As a result, small axis drift, micro-jitter, or modest system latency accumulate over the longer physical path, increasing the visual–proprioceptive mismatch. Hence, the high-gain condition felt more salient despite good accuracy.

Completion time. Completion times increased monotonically from ring 1 to ring 5 for both mechanisms. However, completion time did not correlate with accuracy and primarily reflects travel distance, not remapping quality. We therefore focus on accuracy in the main text; full statistics are in the Supplement.

5.3.5 Conclusion. In general, virtual (re)mapping effectively guides engagement with modest C/D gains. Results also provide some insights: (1) Anchoring a middle ring at C/D = 1.0 and then assigning gains for neighboring rings minimizes extreme gains. (2) Avoiding making the nearest (small gain: premature stops)/farthest (large gain: perceived lag) rings for achieving the desired reconfiguration. Even when gains lie within reported "workable" ranges, tracking issues and action dynamics can degrade performance; and (3) Placing target rings toward the middle of the travel (scaled by ring count) tends to achieve desired reconfiguration without compromising user experience.

5.4 User Evaluation 3: VR Experience

We assess user-reconfigured haptics in a coherent task scenario to gather qualitative feedback on the integrated concept. In particular, we examine whether users can follow the interaction flow and perceive intended differences in weight and elasticity without breaks in immersion while the proxy is reconfigured in real time. We instantiate this in the fishing experience introduced in the application section.

Table 1: Questionnaire on the perceived realism and enjoyment in VR.

	Perceived realism
Q1	The proxy was realistic and natural.
Q2	The environment was realistic and natural.
Q3	Experiences in the virtual environment were consistent with my real-world experiences.
Q4	I felt involved in the content of the virtual environment.
	Perceived enjoyment
Q5	I felt a sense of enjoyment while experiencing the virtual reality content.
Q6	The virtual reality session was fun.
Q7	I want to experience this session again.
Q8	I would recommend this session to others.

5.4.1 Design. Study 3 uses a single-condition, exploratory design (no comparative claim) to assess system-level feasibility. Participants experienced a streamlined fishing story arc in VR, interacting only through the user-reconfigured proxy. Three outcomes (big fish, small fish, no fish) each required users to reconfigure the proxy in real time. We measured the usability using System Usability Scale (SUS) [44] and prepared a custom 7-point scale for the perceived realism [6, 64] and enjoyment [6, 33]. (see Table 1).

5.4.2 Apparatus. The proxy combined 18 unit cells with a rotational handle featuring three locking rings (see Figure 17). We mapped big fish to the farthest ring, small fish to the middle ring, and no fish to the initial engagement position. A Unity scene (Meta Quest 2 via Oculus Link) synchronized proxy states, user actions, and visuals through lightweight modules for calibration, motion update, and state transitions.

5.4.3 Procedure. After consent and demographics, participants donned the HMD and received the user-reconfigured proxy. They completed a brief warm-up (linear engage slide, then reel in/out rotation). A short calibration aligned the virtual rod to the physical proxy (same local-frame method as Study 2). Participants then played a streamlined fishing scenario (cast, reel, pull) while the proxy reconfigured to represent three different outcomes. Think-aloud comments on perceived haptic differences were encouraged. At the end, participants completed SUS and a custom 7-point questionnaire, followed by a short semi-structured interview.

5.4.4 Results. SUS score was 76.2/100 (SD = 11.5, N = 14), which is above the 68-point benchmark; the 95% CI is [68.9, 83.5]. Figure 18 shows that the perceived realism and enjoyment scores were above the scale midpoint across measures. Audio analysis further highlighted three impressions: (1) *Distinguishability.* Participants reported that differences between small- and big-fish outcomes were clear and believable (e.g., *"I did feel the differences...in the pull*

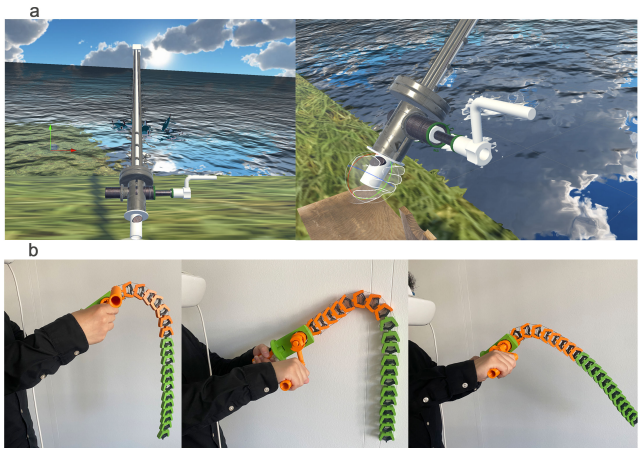

Figure 17: a. VR fishing scenario with the virtual fishing rod. b. Three configurations representing (a) no fish, (b) small fish, and (c) big fish, each producing distinct weight and elasticity experiences.

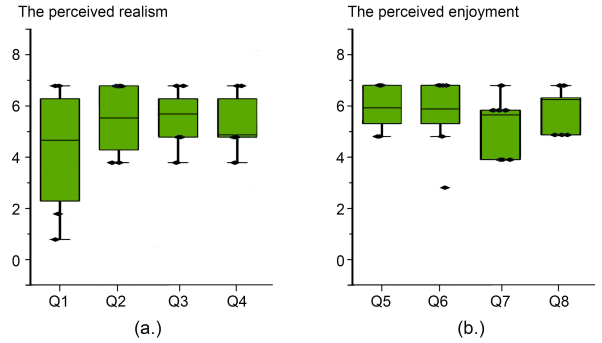

Figure 18: Subjective results on a. The perceived realism. b. The perceived enjoyment.

of my right hand and the grip of my left hand" [P7] and *"when I performed pull back (reel in) actions, I felt like something was being lifted, ... push forward (reel out) actions, ...a gradual feeling of lightening"* [P1]). (2) *Natural transitions.* Participants described the reconfigurations as smooth and integrated into the task (e.g., *"The feeling of holding the handle and spinning was in line with fishing in the real world"* [P9]). (3) *Low cognitive effort.* Some noted that the whole sequence was easy to follow and required little conscious thought (e.g., *"The actions made sense"* [P5]).

5.4.5 Conclusion. Within this single-condition scenario, participants could follow the interaction flow, perceive different outcomes within the fishing task, and perceive reconfiguration as a natural part of the interaction rather than a break in immersion. This study complements the first two evaluations by demonstrating the practical usability and experiential impact of user-reconfigured haptics in a complete VR scenario.

6 Discussion and Limitations

We are convinced that the concept of *user-reconfigured haptics* is a viable and valuable approach to create various haptic experiences without active parts. However, it still has limitations that must be considered and also raises questions for future work.

6.1 Unit Cells and Property Expressivity

6.1.1 Current Limitations. In this work, we exemplify the concept of user-reconfigured haptic proxies by providing modular shape-changing unit cells that can be customized into multiple physical proxies that can further be reconfigured to convey various haptic properties. While this approach offers a certain scalability and adaptability, the expressivity of the current system is limited due to the discrete and finite haptic variation levels. Although a single unit cell can deliver two distinct haptic variations, the overall number of distinguishable haptic variations does not scale linearly with additional unit cells. Attempting to boost haptic expressivity by increasing unit cell counts risks compromising the proxy's lightweight design. Moreover, current multi-cell assemblies primarily exploit shared compression lines, and stiffness modulation is demonstrated at the single-cell level. Tensioning multiple stiffness lines in parallel would require large forces and sustained "force-maintain" effort from the user, which we consider impractical for extended use. Consequently, the expressivity of haptic experiences may be insufficient for highly dynamic VR scenarios, for instance, in scenarios such as gaming that demand an extremely fast and more nuanced range of haptic experiences.

6.1.2 Extension & Future Work. Our unit cell design is only one possible instance in a broader design space of unit cells that exhibit haptic properties. To foster exploring this space, we intentionally designed the unit cell to be parametric and scalable, which eases extension by tailoring the unit cell design to align with various VR scenarios. For example, by minaturizing the size of the unit cell, it is feasible to increase the number of distinguishable haptic property variations without compromising the compact footprint of the proxy. Moreover, *user-reconfigured haptics* is inherently extensible to alternative shape-changing structures, such as shell-based or hinged structures, provided they can support reversible physical transformations. To further enhance the expressivity of haptic properties, future iterations may incorporate advanced materials (e.g., variable-stiffness polymers [2] or shape-memory composites [55]) capable of real-time mechanical transformations. Such material would enable a broader range of haptic property variation. These aforementioned developments aim to create a more continuous spectrum of haptic properties suitable for applications demanding high expressivity, such as gaming and dynamic VR scenarios.

6.2 User Actions

6.2.1 Current Limitations. In our approach, physical reconfiguration is manually driven via rotational and translational rings, which leverages specific user actions (e.g., twisting, pressing, pulling) to transition between different haptic variation levels. This approach, while intuitive and enabling a coherent experience flow, introduces several practical limitations. On the one hand, it necessitates the designer to craft a storyline to embed natural user actions into

VR experiences, imposing additional design complexity, and may limit the applicability of our concept in complex scenarios that require more nuanced user actions. On the other hand, the speed and precision of user-driven reconfigurations are inherently limited. Our concept requires users to engage with these mechanical components directly; however, the imperfections in mechanical components and the inaccuracies in user actions can potentially limit the efficacy of haptic property transitions in fast-paced scenarios. In that case, actuator-based systems might offer finer control over haptic feedback.

6.2.2 Extension & Future Work. Although the current reconfiguration mechanisms can provide reliable and repeatable haptic property transitions, *user-reconfigured haptics* might potentially incorporate gesture-based or multi-touch user interactions, supported by computer vision-based input [15] rather than mechanical triggers, to streamline the reconfiguration process. Additionally, a promising future research direction is to develop hybrid interaction models that combine the manual input with lightweight, energy-harvesting actuation mechanisms, improving both responsiveness and precision. These extensions could reduce user effort and provide dynamic VR haptic experiences in a more lightweight and intuitive manner.

6.3 (Re)Mappings

6.3.1 Current Limitations. Our concept leverages 1-D positional hand redirection along the engagement axis to mask physical transitions and enhance immersion. While these techniques were generally effective, maintaining perfect alignment between visual cues and physical transitions without breaking users' immersion remains a challenge. When performing user actions to transition between different haptic variations rapidly, the drift problems of hand tracking techniques due to the low sensor precision will influence the efficacy of virtual (re)mappings. This is particularly evident in highly interactive VR environments that involve rapid user actions, compromising user immersion or task performance.

6.3.2 Extension & Future Work. To enhance the performance of virtual (re)mapping strategies, our concept could be extended to involve more responsive visual cues and advanced perceptual models [1, 43] that enhance the synchronization between physical and visual cues. Moreover, future research should consider integrating additional sensors, such as inertial measurement units or depth cameras, to improve spatial tracking accuracy and reduce reconfiguration latency. Such improvements can enhance the virtual (re)mapping fidelity, which would not only enhance user immersion but also expand the applicability of *user-reconfigured haptics* to even more dynamic VR experiences.

6.4 Study Design

6.4.1 Current Limitations. Our third study adopts a single-condition, system-level design without a baseline. This lets us focus on the integrated pipeline (reconfigurable proxy, user actions, and remapping), but it also means we cannot make strong comparative claims about realism or enjoyment beyond subjective impressions. In principle, more controlled baselines are possible (e.g., a non-reconfigurable rod with the same form factor, or the same proxy with remapping disabled), but designing, implementing, and counterbalancing these conditions was beyond the scope of this first exploration. We likewise do not measure detection thresholds, sense of agency, or embodiment as in dedicated perception work, so our claims are restricted to feasibility in one implemented application. We therefore explicitly frame Study 3 as an exploratory evaluation rather than a definitive comparison.

6.4.2 Extension & Future Work. Future work can introduce within-class baselines. For example, keeping hardware and user actions constant while toggling specific factors (e.g., remapping on/off) to isolate their contributions. Complementary perception studies could also measure detection thresholds and agency/embodiment in our setting, providing stronger quantitative evidence for the benefits and limits of user-reconfigured haptics.

7 Conclusion

In this work, we introduced *user-reconfigured haptics* as a novel approach to delivering dynamic experiences in VR environments. By enabling users to easily reconfigure proxies, we created a flexible and lightweight solution to convey varied haptic feedback. Our implementation, built on elastic mechanisms, allowed for reversible reconfiguration actions to enrich streamlined VR experiences. Our evaluations, focused on testing the effectiveness of our concept, confirm the usability and effectiveness of *user-reconfigured haptics*. Our proposed applications showcased the versatility of leveraging *user-reconfigured haptics* concept to create dynamic VR haptic experiences. Future research can build on our concept to explore broader applications and improve the technical implementation, paving the way for more sophisticated and interactive haptic experiences in virtual reality.

References

[1] Parastoo Abtahi and Sean Follmer. 2018. Visuo-haptic illusions for improving the perceived performance of shape displays. In *proceedings of the 2018 CHI conference on human factors in computing systems*. 1–13. doi:10.1145/3173574.3173724

[2] Bekir Aksoy and Herbert Shea. 2022. Multistable shape programming of variable-stiffness electromagnetic devices. *Science Advances* 8, 21 (2022), eabk0543. doi:10.1126/sciadv.abk0543

[3] Jason Alexander, Anne Roudaut, Jürgen Steimle, Kasper Hornbæk, Miguel Bruns Alonso, Sean Follmer, and Timothy Merritt. 2018. Grand challenges in shape-changing interface research. In *Proceedings of the 2018 CHI conference on human factors in computing systems*. 1–14. doi:10.1145/3173574.3173873

[4] Lung-Pan Cheng, Li Chang, Sebastian Marwecki, and Patrick Baudisch. 2018. iturk: Turning passive haptics into active haptics by making users reconfigure props in virtual reality. In *Proceedings of the 2018 CHI Conference on Human Factors in Computing Systems*. 1–10. doi:10.1145/3173574.3173663

[5] Lung-Pan Cheng, Patrick Lühne, Pedro Lopes, Christoph Sterz, and Patrick Baudisch. 2014. Haptic turk: a motion platform based on people. In *Proceedings of the SIGCHI Conference on Human Factors in Computing Systems*. 3463–3472. doi:10.1145/2556288.2557101

[6] Lung-Pan Cheng, Sebastian Marwecki, and Patrick Baudisch. 2017. Mutual human actuation. In *Proceedings of the 30th Annual ACM Symposium on User Interface Software and Technology*. 797–805. doi:10.1145/3126594.3126667

[7] Lung-Pan Cheng, Eyal Ofek, Christian Holz, Hrvoje Benko, and Andrew D Wilson. 2017. Sparse haptic proxy: Touch feedback in virtual environments using a general passive prop. In *Proceedings of the 2017 CHI Conference on Human Factors in Computing Systems*. 3718–3728. doi:10.1145/3025453.3025753

[8] Corentin Coulais, Eial Teomy, Koen De Reus, Yair Shokef, and Martin Van Hecke. 2016. Combinatorial design of textured mechanical metamaterials. *Nature* 535, 7613 (2016), 529–532.

[9] Donald Degraen, André Zenner, and Antonio Krüger. 2019. Enhancing texture perception in virtual reality using 3D-printed hair structures. In *Proceedings of*

the 2019 CHI conference on human factors in computing systems. 1–12. doi:10.1145/3290605.3300479

[10] Krzysztof K Dudek, Julio A Iglesias Martínez, Gwenn Ulliac, and Muamer Kadic. 2022. Micro-scale auxetic hierarchical mechanical metamaterials for shape morphing. *Advanced Materials* 34, 14 (2022), 2110115. doi:10.1002/adma.202110115

[11] Martin Feick, Scott Bateman, Anthony Tang, André Miede, and Nicolai Marquardt. 2020. Tangi: Tangible proxies for embodied object exploration and manipulation in virtual reality. In *2020 IEEE international symposium on mixed and augmented reality (ISMAR)*. IEEE, 195–206. doi:10.1109/ISMAR50242.2020.00042

[12] Martin Feick, Cihan Biyikli, Kiran Gani, Anton Wittig, Anthony Tang, and Antonio Krüger. 2023. VoxelHap: A Toolkit for Constructing Proxies Providing Tactile and Kinesthetic Haptic Feedback in Virtual Reality. In *Proceedings of the 36th Annual ACM Symposium on User Interface Software and Technology*. 1–13. doi:10.1145/3586183.3606722

[13] Martin Feick, Niko Kleer, André Zenner, Anthony Tang, and Antonio Krüger. 2021. Visuo-haptic illusions for linear translation and stretching using physical proxies in virtual reality. In *Proceedings of the 2021 CHI Conference on Human Factors in Computing Systems*. 1–13. doi:10.1145/3411764.3445456

[14] Martin Feick, Kora Persephone Regitz, Anthony Tang, and Antonio Krüger. 2022. Designing visuo-haptic illusions with proxies in virtual reality: Exploration of grasp, movement trajectory and object mass. In *Proceedings of the 2022 CHI Conference on Human Factors in Computing Systems*. 1–15. doi:10.1145/3491102.3517671

[15] Weilun Gong, Stephanie Santosa, Tovi Grossman, Michael Glueck, Daniel Clarke, and Frances Lai. 2023. Affordance-based and user-defined gestures for spatial tangible interaction. In *Proceedings of the 2023 ACM Designing Interactive Systems Conference*. 1500–1514. doi:10.1145/3563657.3596032

[16] Eric J Gonzalez, Eyal Ofek, Mar Gonzalez-Franco, and Mike Sinclair. 2021. X-rings: A hand-mounted 360 shape display for grasping in virtual reality. In *The 34th Annual ACM Symposium on User Interface Software and Technology*. 732–742. doi:10.1145/3472749.3474782

[17] Jerônimo Gustavo Grandi, Henrique Galvan Debarba, Luciana Nedel, and Anderson Maciel. 2017. Design and evaluation of a handheld-based 3d user interface for collaborative object manipulation. In *Proceedings of the 2017 CHI Conference on Human Factors in Computing Systems*. 5881–5891. doi:10.1145/3025453.3025935

[18] Jianzhe Gu, Yuyu Lin, Qiang Cui, Xiaoqian Li, Jiaji Li, Lingyun Sun, Cheng Yao, Fangtian Ying, Guanyun Wang, and Lining Yao. 2022. PneuMesh: Pneumatic-driven truss-based shape changing system. In *Proceedings of the 2022 CHI Conference on Human Factors in Computing Systems*. 1–12. doi:10.1145/3491102.3502099

[19] Sebastian Günther, Julian Rasch, Dominik Schön, Florian Müller, Martin Schmitz, Jan Riemann, Andrii Matviienko, and Max Mühlhäuser. 2022. Smooth as steel wool: Effects of visual stimuli on the haptic perception of roughness in virtual reality. In *Proceedings of the 2022 CHI Conference on Human Factors in Computing Systems*. 1–17. doi:10.1145/3491102.3517454

[20] Babak Haghpanah, Ladan Salari-Sharif, Peyman Pourrajab, Jonathan Hopkins, and Lorenzo Valdevit. 2016. Multistable shape-reconfigurable architected materials. *Adv. Mater* 28, 36 (2016), 7915–7920. doi:10.1002/adma.201601650

[21] Douglas P Holmes. 2019. Elasticity and stability of shape-shifting structures. *Current opinion in colloid & interface science* 40 (2019), 118–137.

[22] Jian-Lin Huang, Zhenishbek Zhakypov, Harshal Sonar, and Jamie Paik. 2018. A reconfigurable interactive interface for controlling robotic origami in virtual environments. *The International Journal of Robotics Research* 37, 6 (2018), 629–647. doi:10.1177/0278364918769157

[23] Dohgyu Hwang, Edward J Barron III, ABM Tahidul Haque, and Michael D Bartlett. 2022. Shape morphing mechanical metamaterials through reversible plasticity. *Science robotics* 7, 63 (2022), eabg2171. doi:10.1126/scirobotics.abg2171

[24] Brent Edward Insko. 2001. *Passive haptics significantly enhances virtual environments*. The University of North Carolina at Chapel Hill. doi:techreports/01-017.pdf

[25] Alexandra Ion, Johannes Frohnhofen, Ludwig Wall, Robert Kovacs, Mirela Alistar, Jack Lindsay, Pedro Lopes, Hsiang-Ting Chen, and Patrick Baudisch. 2016. Metamaterial mechanisms. In *Proceedings of the 29th annual symposium on user interface software and technology*. 529–539. doi:10.1145/2984511.2984540

[26] Alexandra Ion, Robert Kovacs, Oliver S Schneider, Pedro Lopes, and Patrick Baudisch. 2018. Metamaterial textures. In *Proceedings of the 2018 CHI Conference on Human Factors in Computing Systems*. 1–12. doi:10.1145/3173574.3173910

[27] Alexandra Ion, Ludwig Wall, Robert Kovacs, and Patrick Baudisch. 2017. Digital mechanical metamaterials. In *Proceedings of the 2017 CHI Conference on Human Factors in Computing Systems*. 977–988. doi:10.1145/3025453.3025624

[28] Yu Jiang, Shobhit Aggarwal, Zhipeng Li, Yuanchun Shi, and Alexandra Ion. 2023. Reprogrammable Digital Metamaterials for Interactive Devices. In *Proceedings of the 36th Annual ACM Symposium on User Interface Software and Technology*. 1–15. doi:10.1145/3586183.3606752

[29] Yu Jiang, Alice C Haynes, and Jürgen Steimle. 2025. Texergy: Textile-based Harvesting, Storing, and Releasing of Mechanical Energy for Passive On-Body Actuation. In *Proceedings of the 38th Annual ACM Symposium on User Interface Software and Technology (UIST '25)*. Association for Computing Machinery, New York, NY, USA, Article 3, 15 pages. doi:10.1145/3746059.3747738

[30] Yijie Jiang, Lucia M Korpas, and Jordan R Raney. 2019. Bifurcation-based embodied logic and autonomous actuation. *Nature communications* 10, 1 (2019), 128. doi:10.1038/s41467-018-08055-3

[31] Hyunyoung Kim, Aluna Everitt, Carlos Tejada, Mengyu Zhong, and Daniel Ashbrook. 2021. Morpheesplug: A toolkit for prototyping shape-changing interfaces. In *Proceedings of the 2021 CHI Conference on Human Factors in Computing Systems*. 1–13. doi:10.1145/3411764.3445786

[32] Robert Kovacs, Eyal Ofek, Mar Gonzalez Franco, Alexa Fay Siu, Sebastian Marwecki, Christian Holz, and Mike Sinclair. 2020. Haptic pivot: On-demand handhelds in vr. In *Proceedings of the 33rd Annual ACM Symposium on User Interface Software and Technology*. 1046–1059. doi:10.1145/3379337.3415854

[33] Jongyoon Lim and Yongsoon Choi. 2022. Force-feedback haptic device for representation of tugs in virtual reality. *Electronics* 11, 11 (2022), 1730. doi:10.3390/electronics11111730

[34] Yuxin Ma, Tianze Xie, Peng Zhang, Hwan Kim, and Seungwoo Je. 2024. AirPush: A Pneumatic Wearable Haptic Device Providing Multi-Dimensional Force Feedback on a Fingertip. In *Proceedings of the CHI Conference on Human Factors in Computing Systems*. 1–13. doi:10.1145/3613904.3642536

[35] John C McClelland, Robert J Teather, and Audrey Girouard. 2017. Haptobend: shape-changing passive haptic feedback in virtual reality. In *Proceedings of the 5th Symposium on Spatial User Interaction*. 82–90. doi:10.1145/3131277.3132179

[36] Zhiqiang Meng, Mingchao Liu, Hujie Yan, Guy M Genin, and Chang Qing Chen. 2022. Deployable mechanical metamaterials with multistep programmable transformation. *Science Advances* 8, 23 (2022), eabn5460. doi:10.1126/sciadv.abn5460

[37] Ken Nakagaki, Yingda Liu, Chloe Nelson-Arzuaga, and Hiroshi Ishii. 2020. Transdock: Expanding the interactivity of pin-based shape displays by docking mechanical transducers. In *Proceedings of the Fourteenth International Conference on Tangible, Embedded, and Embodied Interaction*. 131–142. doi:10.1145/3374920.3374933

[38] Robin M Neville, Fabrizio Scarpa, and Alberto Pirrera. 2016. Shape morphing Kirigami mechanical metamaterials. *Scientific reports* 6, 1 (2016), 31067. doi:10.1038/srep31067

[39] Niels Christian Nilsson, André Zenner, and Adalberto L Simeone. 2021. Propping up virtual reality with haptic proxies. *IEEE Computer Graphics and Applications* 41, 5 (2021), 104–112. doi:10.1109/MCG.2021.3097671

[40] Jin Qiu, Jeffrey H Lang, and Alexander H Slocum. 2004. A curved-beam bistable mechanism. *Journal of microelectromechanical systems* 13, 2 (2004), 137–146. doi:10.1109/JMEMS.2004.825308

[41] Anne Roudaut, Diana Krusteva, Mike McCoy, Abhijit Karnik, Karthik Ramani, and Sriram Subramanian. 2016. Cubimorph: Designing modular interactive devices. In *2016 IEEE International Conference on Robotics and Automation (ICRA)*. IEEE, 3339–3345. doi:10.1109/ICRA.2016.7487508

[42] Neung Ryu, Woojin Lee, Myung Jin Kim, and Andrea Bianchi. 2020. Elastick: A handheld variable stiffness display for rendering dynamic haptic response of flexible object. In *Proceedings of the 33rd annual ACM symposium on user interface software and technology*. 1035–1045. doi:10.1145/3379337.3415862

[43] Yushi Sato, Daisuke Iwai, and Kosuke Sato. 2024. Responsive-ExtendedHand: Adaptive Visuo-Haptic Feedback Recognizing Object Property With RGB-D Camera for Projected Extended Hand. *IEEE Access* (2024). doi:10.1109/ACCESS.2024.3375917

[44] Valentin Schwind, Pascal Knierim, Nico Haas, and Niels Henze. 2019. Using presence questionnaires in virtual reality. In *Proceedings of the 2019 CHI conference on human factors in computing systems*. 1–12. doi:10.1145/3290605.3300590

[45] Adalberto L. Simeone, Eduardo Velloso, and Hans Gellersen. 2015. Substitutional Reality: Using the Physical Environment to Design Virtual Reality Experiences. In *Proceedings of the 33rd Annual ACM Conference on Human Factors in Computing Systems* (Seoul, Republic of Korea) *(CHI '15)*. Association for Computing Machinery, New York, NY, USA, 3307—-3316. doi:10.1145/2702123.2702389

[46] Alexa F Siu, Eric J Gonzalez, Shenli Yuan, Jason B Ginsberg, and Sean Follmer. 2018. Shapeshift: 2D spatial manipulation and self-actuation of tabletop shape displays for tangible and haptic interaction. In *Proceedings of the 2018 CHI Conference on Human Factors in Computing Systems*. 1–13. doi:10.1145/3173574.3173865

[47] Becky Spittle, Maite Frutos-Pascual, Chris Creed, and Ian Williams. 2022. A review of interaction techniques for immersive environments. *IEEE Transactions on Visualization and Computer Graphics* (2022). doi:10.1109/TVCG.2022.3174805

[48] Carolin Stellmacher, Feri Irsanto Pujianto, Tanja Kojic, Jan-Niklas Voigt-Antons, and Johannes Schöning. 2024. Experiencing Dynamic Weight Changes in Virtual Reality Through Pseudo-Haptics and Vibrotactile Feedback. (2024). doi:10.1145/3613904.3642552

[49] Yuqian Sun, Shigeo Yoshida, Takuji Narumi, and Michitaka Hirose. 2019. Pacapa: A handheld vr device for rendering size, shape, and stiffness of virtual objects in tool-based interactions. In *Proceedings of the 2019 CHI conference on human factors in computing systems*. 1–12. doi:10.1145/3290605.3300682

[50] Yichao Tang, Yinding Chi, Jiefeng Sun, Tzu-Hao Huang, Omid H Maghsoudi, Andrew Spence, Jianguo Zhao, Hao Su, and Jie Yin. 2020. Leveraging elastic instabilities for amplified performance: Spine-inspired high-speed and high-force soft robots. *Science advances* 6, 19 (2020), eaaz6912. doi:10.1126/sciadv.aaz6912

[51] Shan-Yuan Teng, Tzu-Sheng Kuo, Chi Wang, Chi-huan Chiang, Da-Yuan Huang, Liwei Chan, and Bing-Yu Chen. 2018. Pupop: Pop-up prop on palm for virtual reality. In *Proceedings of the 31st Annual ACM Symposium on User Interface Software and Technology*. 5–17. doi:10.1145/3242587.3242628

[52] Hsin-Ruey Tsai, Jun Rekimoto, and Bing-Yu Chen. 2019. Elasticvr: Providing multilevel continuously-changing resistive force and instant impact using elasticity for vr. In *Proceedings of the 2019 CHI conference on human factors in computing systems*. 1–10. doi:10.1145/3290605.3300450

[53] Anke Van Oosterhout and Eve Hoggan. 2021. Deformation Techniques for Shape Changing Interfaces. In *Extended Abstracts of the 2021 CHI Conference on Human Factors in Computing Systems*. 1–7. doi:10.1145/3411763.3451622

[54] Yi Wu, Gang Guo, Zhuxuan Wei, and Jin Qian. 2022. Programming soft shape-morphing systems by harnessing strain mismatch and snap-through bistability: A review. *Materials* 15, 7 (2022), 2397. doi:10.3390/ma15072397

[55] Yuliang Xia, Yang He, Fenghua Zhang, Yanju Liu, and Jinsong Leng. 2021. A review of shape memory polymers and composites: mechanisms, materials, and applications. *Advanced materials* 33, 6 (2021), 2000713. doi:10.1002/adma.202000713

[56] Humphrey Yang, Tate Johnson, Ke Zhong, Dinesh Patel, Gina Olson, Carmel Majidi, Mohammad Islam, and Lining Yao. 2022. ReCompFig: Designing dynamically reconfigurable kinematic devices using compliant mechanisms and tensioning cables. In *Proceedings of the 2022 CHI Conference on Human Factors in Computing Systems*. 1–14. doi:10.1145/3491102.3502065

[57] Willa Yunqi Yang, Yumeng Zhuang, Luke Andre Darcy, Grace Liu, and Alexandra Ion. 2022. Reconfigurable Elastic Metamaterials. In *Proceedings of the 35th Annual ACM Symposium on User Interface Software and Technology*. 1–13. doi:10.1145/3526113.3545649

[58] Ruiyang Yin, Depeng Wang, Shufang Zhao, Zheng Lou, and Guozhen Shen. 2021. Wearable sensors-enabled human–machine interaction systems: from design to application. *Advanced Functional Materials* 31, 11 (2021), 2008936. doi:10.1002/adfm.202008936

[59] André Zenner and Antonio Krüger. 2019. Drag:On: A Virtual Reality Controller Providing Haptic Feedback Based on Drag and Weight Shift. In *Proceedings of the 2019 CHI Conference on Human Factors in Computing Systems* (Glasgow, Scotland Uk) *(CHI '19)*. Association for Computing Machinery, New York, NY, USA, 1–12. doi:10.1145/3290605.3300441

[60] André Zenner and Antonio Krüger. 2019. Estimating detection thresholds for desktop-scale hand redirection in virtual reality. In *2019 IEEE Conference on Virtual Reality and 3D User Interfaces (VR)*. IEEE, 47–55. doi:10.1109/VR.2019.8798143

[61] André Zenner and Antonio Krüger. 2017. Shifty: A Weight-Shifting Dynamic Passive Haptic Proxy to Enhance Object Perception in Virtual Reality. *IEEE Transactions on Visualization and Computer Graphics* 23, 4 (2017), 1285–1294. doi:10.1109/TVCG.2017.2656978

[62] André Zenner, Kristin Ullmann, and Antonio Krüger. 2021. Combining dynamic passive haptics and haptic retargeting for enhanced haptic feedback in virtual reality. *IEEE Transactions on Visualization and Computer Graphics* 27, 5 (2021), 2627–2637. doi:10.1109/TVCG.2021.3067777

[63] Xuan Zhang, Yue Wang, Zhihao Tian, Manar Samri, Karsten Moh, Robert M McMeeking, René Hensel, and Eduard Arzt. 2022. A bioinspired snap-through metastructure for manipulating micro-objects. *Science Advances* 8, 46 (2022), eadd4768. doi:10.1126/sciadv.add4768

[64] Kening Zhu, Taizhou Chen, Feng Han, and Yi-Shiun Wu. 2019. Haptwist: creating interactive haptic proxies in virtual reality using low-cost twistable artefacts. In *Proceedings of the 2019 CHI Conference on Human Factors in Computing Systems*. 1–13. doi:10.1145/3290605.3300923